First-principlesStudy of Rare Earth BasedPerovsites$XAlO_3$ (X=Sm, Eu, Gd)for Optoelectronic and Renewable energy Applications

Tariq Usman[a], Salman Ali Khan[a], Asif Ilyas[a]

Zhejiang University, Hangzhou 310027, P. R. China

Corresponding Author; Asif Ilyas

Abstract

First-principles method based on density functional theory calculations are employed for investigating the electronic, optical and thermoelectric properties of $XAlO_3$ (X= Sm, Eu, Gd) for energy-devices applications. The spin-polarized electronic spectra of $XAlO_3$ depicts their half metallic nature since mere the spin up channel crosses the fermi level. Further, the optical features for instance, the dielectric functions, refractive index, absorption coefficient, extinction coefficient, optical conductivity, reflectivity, and energy loss function are studied which predict that these compounds can be best candidate materials for the ultraviolet-region based optoelectronic and energy devices. Thermoelectric properties in term of electrical and thermal conductivity, and figure of merit show higher values of thermoelectric charecters which is extremely significant for optoelectronic devices. Interestingly, the positive value of Seebeck coefficient indirectly depict that $XAlO_3$ is a p-type materials.

Keywords

Density functional theory; Optoelectronic; Solar cells; Renewable energy; Thermoelectric efficiency

1. Introduction

It is eminent that perovskite materials find many applications and are of great interest in material science and technology due to their simple crystal structure. Previous studies shows that these materials display various properties such as magnetic, electronic, electric, piezoelectric, optical, catalytic and magneto-resistive properties. They got great interest in earth sciences, because $MgSiO_3$ and $FeSiO_3$transforms to a perovskite structure with Pbnm symmetry at high-pressures and temperatures. It is believed that the bulk of the earth's lower mantle is formed from perovskite materials [1,2]. Such material properties make them feasible in the development and fabrication of many technological devices. The immense interest has been paid by researchers to study these materials properties to get information in order to modify the performance of devices in future modeling. The structure of perovskite is the most frequently encountered in solid-state physics, and has great importance due to their prospective application as solar-cell absorbers [3-5] topological insulators [6] and even superconductors [7]. The lead base halide perovskite compound was discovered for the first time as a solar cell absorber for photovoltaic device applications [8]. In recent times, perovskite materials have achieved 24.2% the power-conversion efficiencies (PCEs) [9], having stunning photovoltaic properties and superb optical absorption [10]. Due to high PCEs, perovskites have attracted noticeable attention and is intended finally at the commercial applications for solar power-conversion.

On the basis of the composition and tilted degree of polyhedral at room temperature, the perovskite shows different crystal structures, for instance cubic, monoclinic, tetrahedral,

hexagonal, and rhombohedral structure etc. Among these, perovskites having a cubic structure with general chemical formula ABX_3 is occurring very commonly and incredibly significant representative among the inorganic compounds. It consists of 3-D structure of BX_6 octahedron with corner sharing, where A-cation is surrounded with twelve equidistant atoms and thus has a coordination number of twelve [11]. It is broadly speaking that, this type of perovskites has a high potential for the field of optoelectronics and also for a variety of device applications due to its simple crystal structure and unique ferroelectric and dielectric properties [12,13]. It also attracted enormous attention due to their competent use in gas separation, fuel cells, chemical reactors, high temperature superconductivity, ferroelectricity, piezoelectricity and etc [14,15].The physical properties of these materials are a part of many research and reveals significant properties from theoretical and experimental point of view, for example superconductivity, ferroelectricity, magnetic and optical properties [14, 16].

Rare earth aluminates perovskites $XAlO_3$ (R=La, Ce, Pr, Nd, Pm, Sm, Eu, Gd) are widely used as substrate materials for the epitaxy of HTSC and CMR materials, and GaN films [17], as materials for solid oxide fuel cells [18], as active and passive laser media [19], as scintillators [20], and as microwave dielectric materials [21]. Single crystals of $YAlO_{3,}$ doped with Nd, Tm, and Er, are well known as laser media [22]. As prospective laser materials, also $LuAlO_{3:}$Nd and $TbAlO_3$ are considered [23]. Most of the rare earth aluminates achieve dielectric permittivity with ‘high-quality factor’ suitable for applications in dielectric resonators and substrates for microwave components [24]. Cerium-containing oxides (including perovskites) are of great

interest in the chemistry of modern materials for efficient lighting as well as in the technology of weapons-grade Pu in mixed-oxide fuel. Rare earth aluminates, such as $DyAlO_3$, $ErAlO_3$, and $HoAlO_3$, are paramagnetic down to very low temperatures (typically a few Kelvin) and on ordering, they arrange anti-ferromagnetically. This fact together with large values of magnetic moments typical forrare earth elements makes them suitable for working bodies in magnetic refrigerators for the production of liquid helium [25]. Hence, from these studies we get that many efforts have been made to investigate diverse properties of cubic $XAlO_3$ compounds, while inspired us to study their properties for technological purpose. In this work, we present spin polarized investigation of electronic, optical, and thermoelectric properties of $XAlO_3$ (X = Sm, Eu, Gd) compounds by first-principles method with this hope to examine their possibility for optoelectronic and photovoltaic applications. So, we hope that this study will offer a theoretical support to the future studies, and further it will be handy to guide experimental studies for optoelectronic and photovoltaic applications.

2. Computational Detail

In the present calculations, the full-potential linearized augmented plane wave method (FP-LAPW) [26] is used to solve Kohn-Sham equations [27] as executed in the WIEN2K code [28]. For computation, the adopted method is based on density functional theory (DFT) [29,30] which has been considered to be one of the precise methods for electronic and optical properties of different materials. For exchange-correlation, the generalized gradient approximation (GGA) and GGA+U approximation are used to compute the total energy, and the strong Coulomb repulsion between localized d and f orbitals is treated by adding a

Hubbard term to the effective potential, leading to an improved description of correlation effects. Also, the modified Becke-Johnson (mBJ) [31] approximation is included for the effective representation of the band gap. The valence electrons are treated semi-relativistically, while core electrons are treated fully relativistically in these calculations. For convergence, the muffintin radii (RMT) are chosen in such a way that there is no charge leakage from the core. By using modified tetrahedron method [32], the integrals over the Brillouin zone are executed upto 35 k-points, while for optical properties 75 k-points are chosen for Brillouin zone integration in the irreducible part of the Brillion zone (IBZ). The self-consistent calculations are considered to be converged when the total energy is stable within 0.1 mRy.

2. Results and Discussion

2.1 Structural and Electronic Properties:

The crystal structure of $XAlO_3$ (X = Sm and Eu) is cubic, where six oxygen atoms form octahedron with Al in its center. A 2*2*2 supercell is shown in the Fig. 1, where the X cation occupies the corners of the unit cell. The negative ground state energy confirms its structural stability. The optimized lattice constants conrrespong to the ground state energy a=b=c. The lattice parameter for different X cation are slightly different due to their different atomic radii.

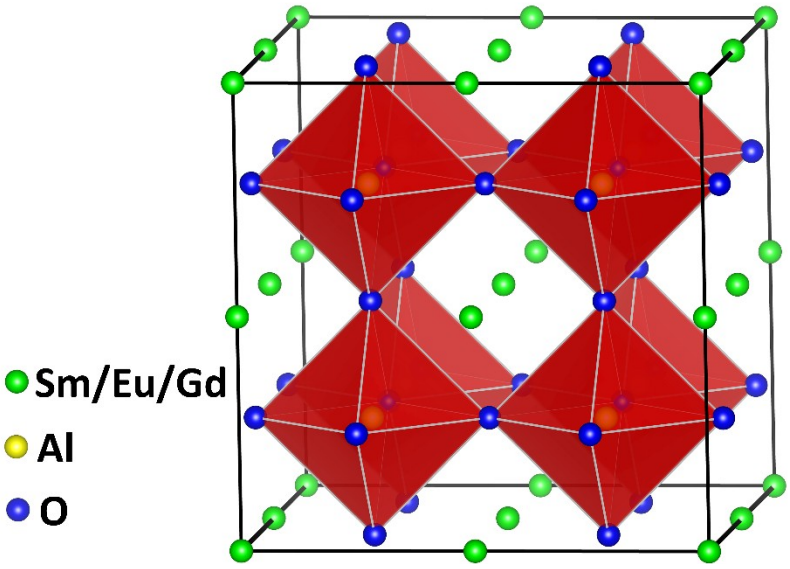

Fig. 1. (color online)A 2∗2∗2 crystal structure of $XAlO_3$ (X = Sm, Eu, Gd), where different atoms are represented with different colors are shown. Each octahedron contains three oxygen atoms at their ages with one Al atom setting in its center. The unit cell of $XAlO_3$ is formed by an octahedron with four atoms at its corner (Note: four atoms of X element constitutes one atom).

To dig into the details of the electronic properties of $XAlO_3$ compounds, we computed the spin-polarized band structures (BS) and the electronic density of states (DOS) regarding $XAlO_3$ (X = Sm, Eu and Gd)as shown in the Fig. 1(a-b). The spin-up (↑) and spin-down (↓) bands are represented by light green and red colors respectively. The size and valance shell electronic configurations of the X cation makes them unique from each other regarding electron properties. Interestingly, GGA and GGA+U both schemes demonstrate similar qualitative results.

The band structures depend upon their electronic configurations. $XAlO_3$ with X= Sm and Eu cations conduct via spin-up channel whereas their spin-down channels remains insulating. On the contrary, the presence of Gd cation makes both the channels insulating. It can be seen from the Fig. 2 (i-l), that it is half semiconductor as the the top of the valance band is contributed by spin channel, while the bottom of the conduction band is contributed by spin down channel. The different behaviors of the electronic structureis rooted in different electronic configurations of the three cations. For example, the d-orbital of the former (X= Sm and Eu) is completely filled, while the Gd has $5d^1$ electronic configuration. Importantly, the spin-up channel regarding X= Sm and Eu are hundred spin polarized. Such types of half metals can play an important role for the development of spintronic devices. The band structures are very interesting since the spin-up marginally crosses the fermi level for X= Sm and Eu. In these compound, it can be useful to alters their electronic properties because a small amount of strains can possibly transform them from half metals to semiconductor.

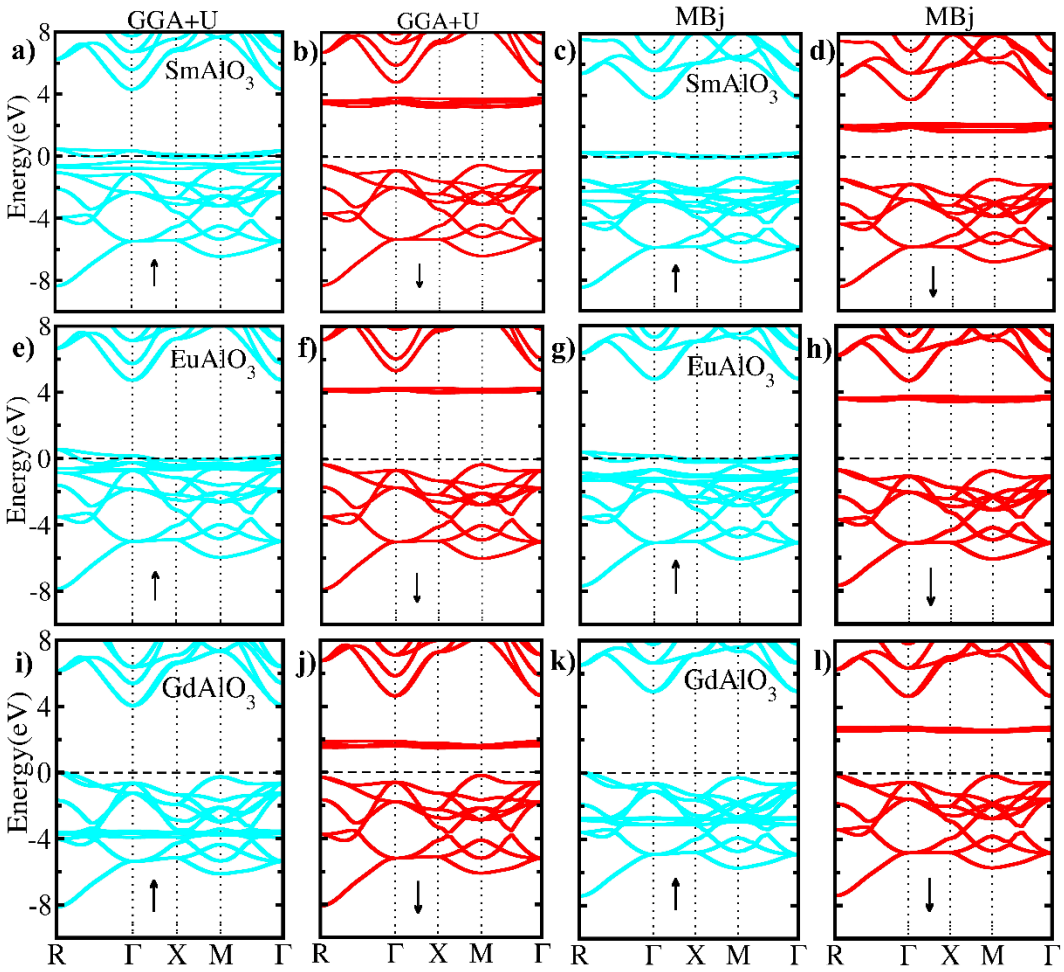

Fig. 2. (Color online) Spin-polarized band structures of $SmAlO_3$, $EuAlO_3$ and $GdAlO_3$ calculated by MBJ and GGA+U method are shown (a-l).

To further investigate the electronic properties of the these compounds, we computed the the total densities of states (TDOS) as well as partial density of states (PDOS). The PDOS shown in Fig. 3. illustrate that the states located around the Fermi level originate from the hybridization of the Sm f-orbital, Eu f-orbital with O-p atomic orbitals. Neverthless, GGA and GGA+U both approach depict that the major contribution in the hybridization comes from Sm-f and Eu-f orbital.

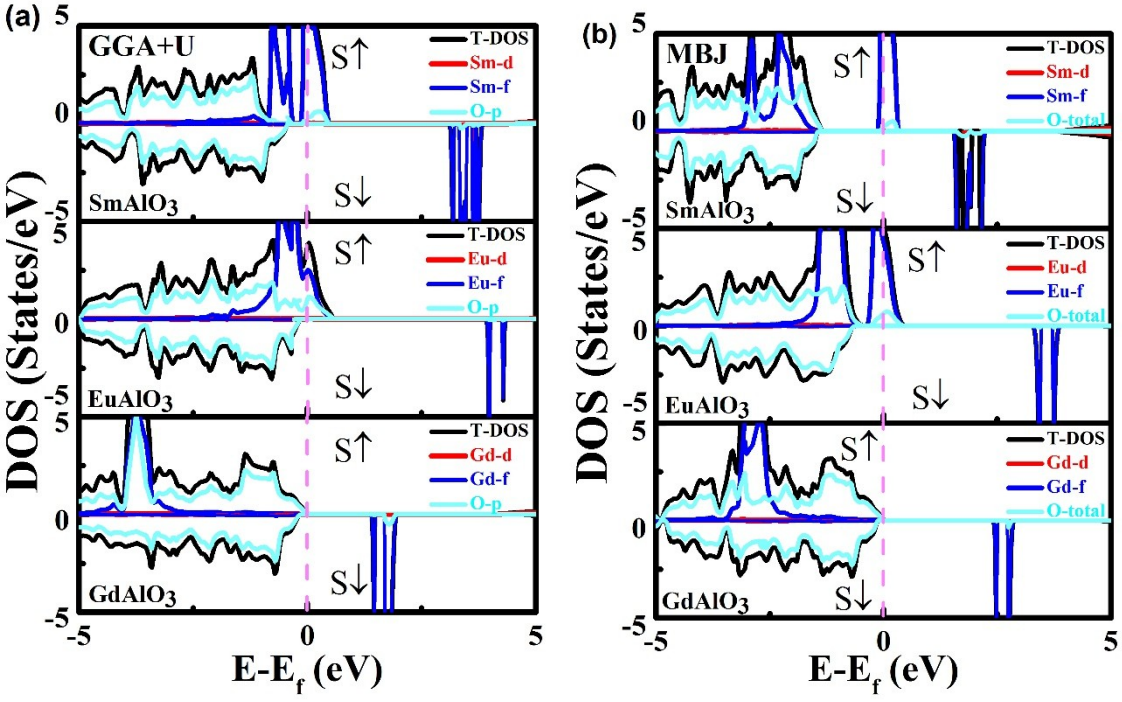

Fig. 3. (Color online) Spin-polarized total and PDOS of $SmAlO_3$, $EuAlO_3$ and $GdAlO_3$are calculated by MBJ and GGA+Umethod as shown in (a-b).

3.2Optical Properties:

The optical spectra givepreciousknowledgeregarding the innerconfiguration of materials. It is intentlyconnectedwith electronic properties to identify the optoelectronic nature of the material for various applications. The optical properties are normallyacquiredthrough dielectric function $\varepsilon(\omega) = \varepsilon_1(\omega) + i\varepsilon_2(\omega)$ which elucidate the medium optical reactionto incident energies of photon.The imaginary part $\varepsilon_2(\omega)$ in dielectric function is incredibly significant, which is intimatelycorrelated to material electronic band spectrum and spell out the

absorptionperformance.By means of Kramers-Kronig relations [33], the real part $\varepsilon_1(\omega)$ is eliminated from the imaginary part, whereas the rest of the optical features are computed as of dielectric function parts, for instance refractivity, absorption spectra, loss-function, reflectivity, and conductivity.

We presented all the computed dielectric functions of $XAlO_3$(X= Sm, Eu, Gd) compounds in Fig. 4. The parts of the dielectric function such as real $\varepsilon_1(\omega)$ and imaginary $\varepsilon_2(\omega)$ for $XAlO_3$ compounds as a fuction of photon energy are depicted in Fig.4(a,b) in 0-30 eV energy range.The real part $\varepsilon_1(\omega)$ provides useful information regarding the electronic polarizability of a material. At zeroω=0, we get the static dielectric constant as $\varepsilon_1(0)$ = 38, 43, 4 for $SmAlO_3$, $EuAlO_3$and $GdAlO_3$ respectively.It decreases by increases the frequency and eventually become negative for $SmAlO_3$(-3.5)and $EuAlO_3$(-7.3)at 0.35 eV,while for $GdAlO_3$ (-1.0) at 20-22 eV. Again at 7.2, 7.5, and 7.8 eV, the magnitude of $\varepsilon_1(\omega)$ increases from zero frequency limit to the peak value (6.1, 5.8, and 6.5) for all these compounds. As soon as the values of real part $\varepsilon_1(\omega)$ acquires negative values, then the material displays metallic behavior, or else, represents dielectric behavior. The other part of thedielectric function is the most important parameter called as imaginary part $\varepsilon_2(\omega)$, which gives some significant information about the diverse interband transitions between the valence and conduction bands, as shown in Fig. 4(b). From the figure, it can be clearly seen that higher peaks for $SmAlO_3$ and $EuAlO_3$ occurs at 0.13 and 0.16 eV, while the higher peak for $GdAlO_3$ is located at 7.7 eV. The critical points of $\varepsilon_2(\omega)$ for all compounds are around 0.07, 0.09, and 2.7 eV, corresponding to the bandgap at equilibrium. The origin of these peaks is lying in the interband transitions, which arelinkedwith the material density of states as

shown in Fig. 2. The emergence of peaks are due to the electrons transitionfrom the valence to conduction band.

The refractive index n(ω) among these optical functions is a pivotal parameter for elucidating the materials optical charecteristics, and has a significant impact on optical devices,for example solar cells and detectors [34] as shown in Fig. 4(c). We found thatat zero frequency limit,the values of the refractive index are6.6, 6.8 and 2.0 for $SmAlO_3$, $EuAlO_3$, and $GdAlO_3$. The maximum value of refractive index are2.3, 2.7, and 2.5 located at 9.7, 10.9, and 9.9 eV, respectively.Fig. 4 (d) represents the extension coefficient k(ω) parameter which describes the electromagnetic waves attenuation in materials. From figure, the critical points of k(ω) are 0.1, 0.1, and 2.7 eV for all these compounds. We also calculatedthe maximum height of k(ω)3.2, 4.0, 1.2 (for $SmAlO_3$ and $EuAlO_3$) at 0.25 whereas 0.28 for $GdAlO_3$at8.8 eV. The absorption coefficient α(ω) is shown in Fig. 4(e), and their critical points are 0.1, 0.14, and 2.4 eV for $SmAlO_3$, $EuAlO_3$, and $GdAlO_3$. The maximum height α(ω) for the given compounds are 380, 377, 340 which occurs at 26.3, 26.2, and 28.6 eV, respectively. In the energy range of 7-30eV, they react very strongly to the incoming photons.Fig. 4(f) presents the optical conductivity σ(ω) of $XAlO_3$(X= Sm, Eu, Gd), which beginsreplying to the energy field from 0.1, 0.12, and 2.7eV. The higher optical conductivity for the given compounds are obtained at 24.9, 25.3 and 27.0 eVwith a magnitude of 12.0, 10.5, and 9.4 Ω^{-1} cm^{-1}. In Fig. 4(g,h), the reflectivity spectra R(ω) and electron energy loss spectra L(ω) are displayed. In the given figure, the function R(ω) is animperative parameter that characterizes the part of reflected energy at the interfaces, where L(ω)portrays the loss of energy of a fast electron as they pass through a material. We obtained the value atzero

frequency limit of reflectivity R(ω) is 0.58, 0.57, and 0.1for $SmAlO_3$, $EuAlO_3$, and $GdAlO_3$. The maximum reflection peaks for the given compounds are0.62, 0.59 and 0.69 occurs at 28.8, 28.9 and 29.9 eV, respectively. The highest peaks of L(ω) are 10.0, 8.5, and 6.5 occurs at 31.4, 31.3 and 31.8 eV for the given compounds, where these peaks show the attributeslinkedthrough theplasma resonance. So, the maximum resonant loss of energy isnoticed at these peaks.

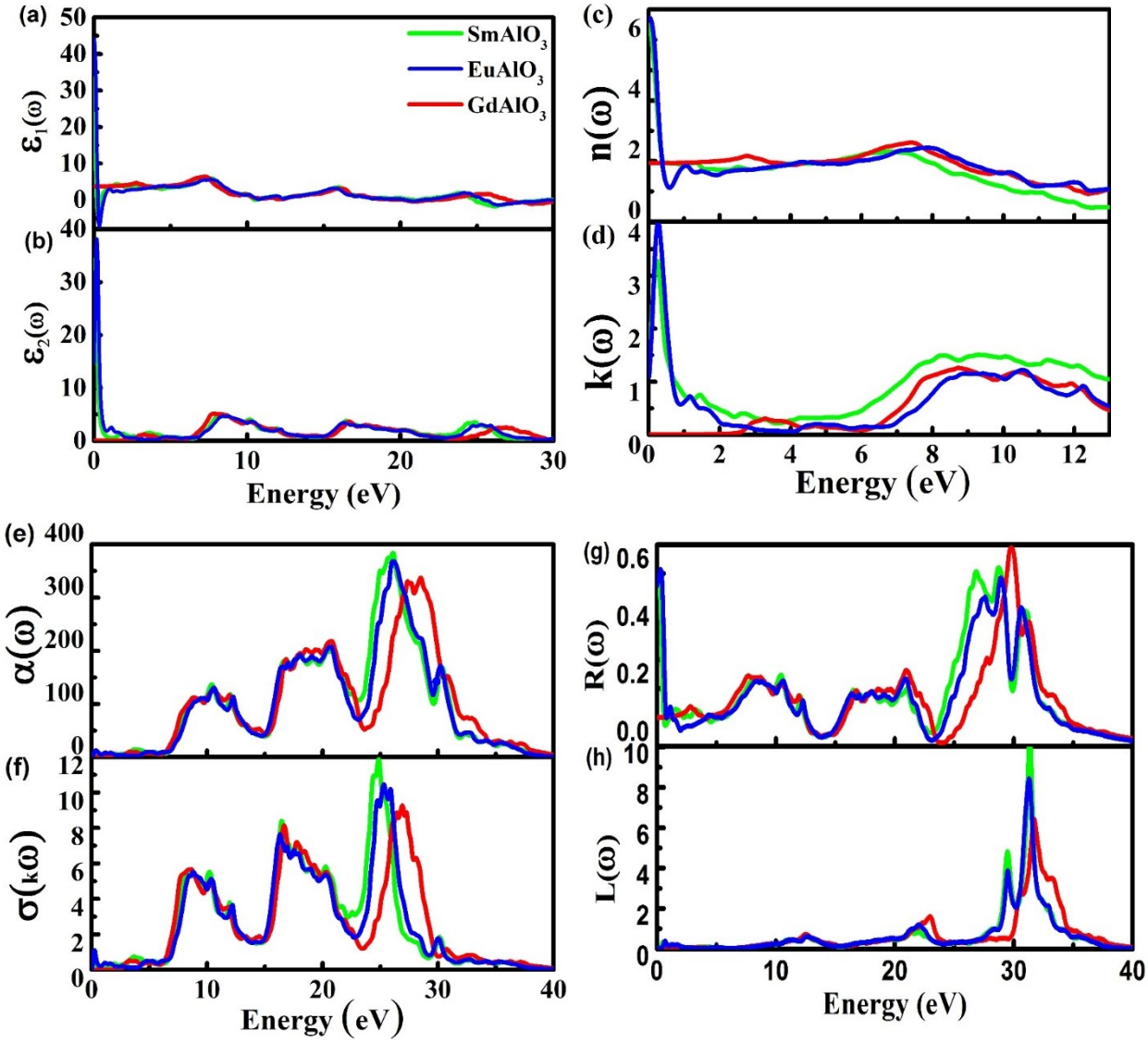

Fig. 4. (Color online) Dielectric function; (a) real part $\varepsilon_1(\omega)$ and (b) imaginary part $\varepsilon_2(\omega)$ (c) refractive Index $n(\omega)$ and (d) extinction coefficient $k(\omega)$ **(e)** optical conductivity $\sigma(\omega)$ and (f) absorption coefficient $\alpha(\omega)$ (g) Reflectivity spectra $R(\omega)$ and (h) electron energy loss spectra $L(\omega)$

3.3Thermoelectric Properties:

The half metallic materials has attreacted great research interest in recent times for thermoelectric applications in various optoelectronic, spintronic, and magnetoelectronic devices. By Boltzmann transport theory, the rare-earth based perovskites $XAlO_3$ (X= Sm, Eu, Gd) thermoelectric properties are calculated within the constant relaxation time (τ) as employed in the BoltzTrap Code [35,36]. For $XAlO_3$ (X= Sm, Eu, Gd) compounds, the imperative thermoelectric characters are described in terms of essential transport properties,resemblingSeebeck coefficient, electrical conductivity, thermal conductivity, and figure of merit as a function of temperature, as shown in Fig. 5.

For thermoelectric materials, the Seeback coefficient playing an essential role in building thermoelectric efficiency and representing the difference of voltage ratio between thermal contacts of a metals to temperature difference. Fig. 5(a) showing the Seebeck coefficient for $XAlO_3$ compounds as a function of temperature dependence.The Seebeck coefficient increases for $XAlO_3$ compounds as suggested by the figure with the increase in temperature. For $SmAlO_3$ and $GdAlO_3$, the

Seebeck coefficient increases at a faster rate upto 800k, but for $EuAlO_3$ it linearly increases.After 600K, the Seebeck coefficient for $EuAlO_3$ is going to consistency up to 800 K due to potential barrier keeped up by the flow of charge carriers at high temperature. In all these compounds, the potential barrier for $EuAlO_3$ is higher as compared to $SmAlO_3$ and $GdAlO_3$ may be due to fast collision rate of charge carriers.The higher values of Seebeck coefficient are 0.14, 0.09, and 0.13 mV/K at 800K for $SmAlO_3$, $EuAlO_3$, and $GdAlO_3$.The Charge carriers type choose that whether the Seebeck coefficient is positive or negative.Hence, our computed Seebeck coefficient for the given compounds is positive and confirmed from the positive value in the temperature range 150- 800K, which make certain the p-type materials.

Further, we calculated the electrical conductivity for rare-earth based $XAlO_3$ perovskites as a function of temperature which are shown in Fig. 5(b). The movement of electrical charge in a material is the electrical conductivity which helps in sympathetic the relation between charge carrier and electric current. For good thermoelectrical materials, the electrical conductivity is high which decreases the joule-heating effect [37]. It is obvious from the figure that the electrical conductivity increases with the increase in temperature for all compounds due to increase in kinetic energy of carriers which may causes an increase in conductivity, but for $EuAlO_3$, first the conductivity increases upto 700K, than it decreases.The electrical conductivity value at room temperature are 5.22×10^{19}, 6.67×10^{19}, and $5.36\times10^{19}(\Omega ms)^{-1}$ for $SmAlO_3$, $EuAlO_3$, and $GdAlO_3$ compounds, while their higher values approximately at 800K are 5.74×10^{19}, 7.04×10^{19}, and $6.05\times10^{19}(\Omega ms)^{-1}$for the same compounds, which show that $EuAlO_3$ has higher electrical

conductivity may be due to $EuAlO_3$ provides more free carriers as compared to $SmAlO_3$ and $GdAlO_3$. It is noticeable that, the rise in electrical conductivity with varying temperature show that these compounds have good potential that could be used efficiently for thermoelectric applications.

At different temperature, we also calculated the thermal conductivity which is very significant for elucidation of thermoelectric materials performence. A good thermoelectric materials performance is also characterized from their low thermal conductivity [38,39]. The thermal conductivity as a function of temperature is shown in Fig. 5(c). The plot of thermal conductivity show that, as temperature increases, thermal conductivity also increases for $XAlO_3$ compounds due to thermal excitation of charge carriers which conducting more heat. For $EuAlO_3$, the thermal conductivity is smaller at heigher temperature in contrast to $SmAlO_3$ and $GdAlO_3$. At room temperature, their values are minimum, and incrases with the rise in temperature to 1.77×10^{14}, 1.25×10^{14}, and 1.75×10^{14} W/mKs at 800K which decreases the thermoelectric efficiency and adopts metallic behaviour. So, our thermal conductivity results also show that the given compounds are efficiently used as thermoelectric materials.

Furthermore, we analyzed the figure of merit (ZT) to examine the efficiency of the given compounds at different temperature which is deduced from the figure of merit as shown in Fig. 5 (d). The Plot of ZT show that, as temperature increases then figure of merit also increases and reaches to the maximum values 0.51, 0.44, and 0.50 for $SmAlO_3$, $EuAlO_3$, and $GdAlO_3$ at 800K. The values of the figure of merit at 300Ktemperarature are 0.2, 0.18, and 0.18 for $SmAlO_3$, $EuAlO_3$, and $GdAlO_3$. Among the given compounds, SmAlO3 has the heighest figure of merit at heigher

temperature. The increase in figure of merit is due to variation in indirect bandgap with temperature, because the bandgap decreases with increase in temperature that enhances the figure of merit and electrical conductivity increases. From increasing figure of merit and decreasing thermal conductivity the thermoelectric materials efficiency can be enhanced. Hence, our studied compounds can be proficiently used for optoelectronic and thermoelectric device applications.

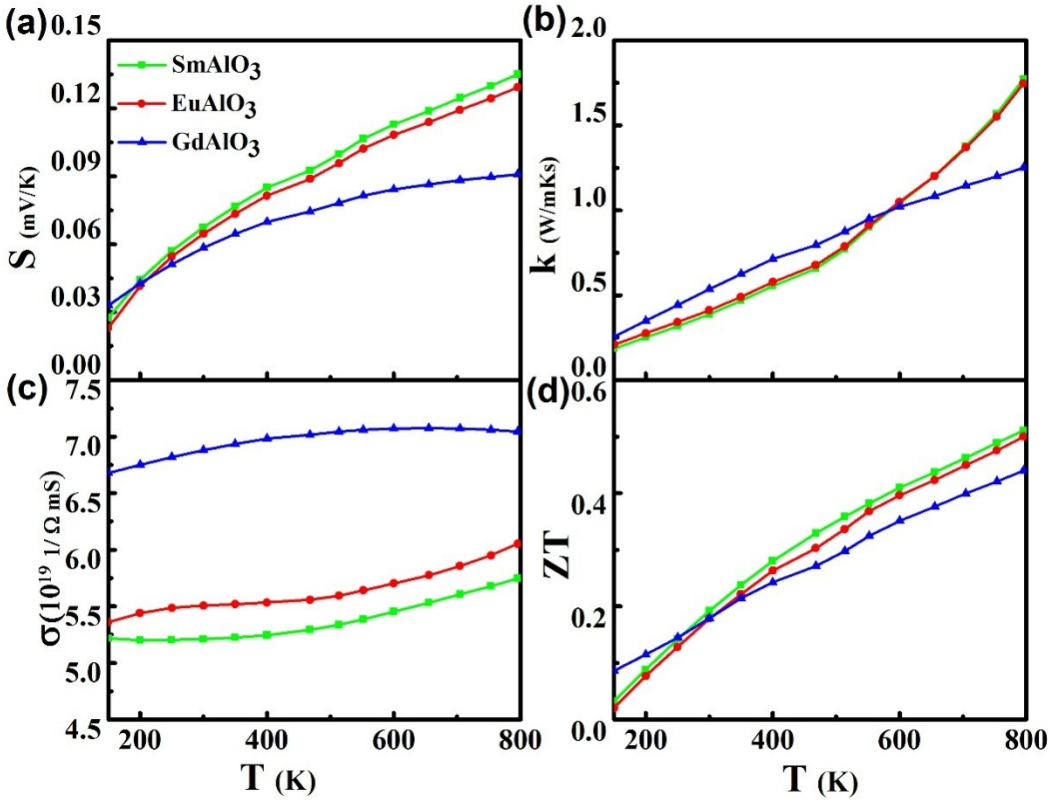

Fig. 5. (Color online) Thermoelectric properties of $XAlO_3$ (X = Sm, Eu, Gd) compounds as a function of temperature dependence. (a) See beck coefficient (b) electrical conductivity (c) thermal conductivity (d) figure of merit (ZT).

Conclusions

In summery, we predict the electronic, optical, and thermoelectric properties of rare earth based perovskites $XAlO_3$(X= Sm, Eu, Gd) compounds viafirst-principles calculations by employing GGA+U and mBJ potentials.Spin polarized calculation with both mBJ and GGA+U approximations are carried to investigate electronic properties of $XAlO_3$, which shows that it not only depends on the electronic configuration but also on the size of the atom. Therefore,$XAlO_3$(X= Sm, Eu) depictshalf metallicity. On the contrary, $GdAlO_3$ owns semiconducting nature. It can be seen in the PDOS and band structures that $XAlO_3$(X= Sm, Eu)create states at the fermi level due to their half metallic nature. However, the spin down channels remain insulating for these compounds with a sizable band gap (2.6 eV and 2.2 eV). Further, the optical features, for instance dielectric functions, refractive index, absorption coefficient, extinction coefficient, optical conductivity, reflectivity, and energy loss function are studied and predict that these compounds can be used efficiently in the ultraviolet region based optoelectronic and energy devices. To get further insight, thermoelectric properties in term of electrical and thermal conductivity, Seebeck coefficient, and figure of merit have been studied by Boltzmann transport theory and predict the higher values of thermoelectric charecters and positive value of Seebeck coefficient show that $XAlO_3$ is a p-type materials, while figure of merit show that it can be significant for thermoelectric as well optoelectronic devices.Hence, these compounds have excellent optical absorption in the ultraviolet range and high thermoelectric characters due to their stable

structure. They can be candidate materials for solar cells and high power conversion efficiency.

References:

1. R. Terki, H. Feraoun, G. Bertrand, H. Aourag, Phys. Stat. Sol. (b) 242 (2005) 1054.
2. C.E. Runge, A. Kubo, B. Kiefer, Y. Meng, V.B. Prakapenka, G. Shen, R.J. Cava, T.S. Duffy, Phys. Chem. Miner. 33 (2006) 699.
3. I. Chung,B.Lee,J. He,R.P.HChang,G. Kanatzidis, all-solid-state dye-sensitized solar cells with high efficiency Nature 485 (2012)486.
4. M.M. Lee, J. Teuscher, T. Miyasaka, T.N. Murakami, H.J. Snaith,Eficient hybrid soler cells besed on meso-superstructuredorganometal halide perovskites Science 338 (2012) 643.
5. J. Burschka, N. Pellet, S.J. Moon, R. Humphry-Baker, P. Gao, M.K. Nazeeruddin, M. Gratzel,Sequential deposition as a route to high performance perovskite-sensitized soler cells Nature 499 (2013) 316.
6. H. Jin, J. Im, A.J. Freeman, Topological insulator phase in halide perovskite structures Phys. Rev. B 86 (2012) 121102.
7. Y. Takahashi, R. Obara, Z.-Z. Lin, Y. Takahashi, T. Naito, T. Inabe, S. Ishibashi, K. Terakura, Charge-transport in

tin-iodide perovskite $Ch_3NH_3SnI_3$:origin of high conductivity Dalton Trans. 40 (2011) 5563.

8. A. Kojima, K. Teshima, Y. Shirai, T. Miyasaka, Organometal halide perovskites as visible-light sensitizers for photovoltaic cells J. Am. Chem. Soc. 131 (2009) 6050.
9. NREL. Best research-cell efficiencies. https://www.nrel.gov/pv/assets/pdfs/best-researchcell-efficiencies190416.pdf. Accessed April 1, 2019.
10. G. Giorgi, JI. Fujisawa, H. Segawa, K. Yamashita,Smallphotocarrier effective masses featuring ambipolar transport inmethylammonium lead iodide perovskite: a density functional analysis J PhysChem Lett. 4 (2013) 4213.
11. T. Wolfram, and S. Ellialtioglu, Electronic and Optical Properties of d-Band Perovskites: Cambridge University Press, 2006.
12. Ramesh, R., Spaldin, N.A.: Multiferroics: progress and prospects in thin films . Nat. Mater. 6, 21–29 (2007).
13. Huang, Y.H., Dass, R.I., Xing, Z.L., Goodenough, J.B.: Double perovskites as anode materials for solid-oxide fuel cells. Science 312, 254–257 (2006).
14. G. Murtaza, I. Ahmad, B. Amin, A. Afaq, M. Maqbool, J. Maqssod, I. Khan, M. Zahid, Opt. Mater. 33 (2011) 553.
15. Z. Ali, I. Ahmad, B. Amin, M. Maqbool, G. Murtaza, I. Khan, M.J. Akhtar, F. Ghaffor, Physica B 406 (2011) 3800.
16. J.M.D. Coey, M. Viret, S.V. Molnaacuter, Adv. Phys. 48, 167 (1999).
17. K. H.Young and D. D. Strother, Phys. C (Amsterdam, Netherlands), **208**, 1 (1993).
18. P. Hohenberg and W. Kohn, Phys. Rev., **136**, 864-868 (1964).

19. P. Blaha, K. Schwarz, and J. Luitz, ISBN 3-9501031-0-4, (2001).
20. J. P. Perdew and W. Yue, Phys. Rev. B, **33**, 8800 (1986).
21. F. Tran and P. Blaha, Phys. Rev. Lett., **102**, 226401 (2009).
22. A. A. Kaminskii, Phys. Status Solidi A, **148**, 9 (1995).
23. H. A. Abu Safia, Opt. Commun., **139**, 212 (1997).
24. C.L. Huang and Y.C. Chen, Mater. Res. Bull, **37**, 563(2002).
25. K.A. Gschneidner, C.G. Bünzli and V.K. Pecharsky, editors: Handbook on the Physics and Chemistry of Rare Earths, Vol. 39, Netherlands: North-Holland (2009).
26. Kohn, W.; SHAM, L.J. Self-Consistent Equations Including Exchange and Correlation Effects. Phys. Rev. **1965**, 140, A1133. [Z. Wu, R.E. Cohen, Phys. Rev. B 73 (2006) 235116].
27. W. Kohn, L.J. Sham, Phys. Rev. 140 (1965) A1133.
28. P. Blaha, K. Schwarz, G.K.H. Madsen, D. Kvasnicka, J. Luitz, WIEN2k, An Augmented Plane Wave plus Local Orbitals Program for Calculating Crystal Properties, Vienna University of Technology, Vienna, Austria, 2001; K. Schwarz, P. Blaha, G.K.H. Madsen, Comput. Phys. Commun. 147 (2002) 71.
29. Hohenberg, P.; Kohn,W. Inhomogeneous Electron Gas. Phys. Rev. 1964, 134, B864.
30. Blaha, P.; Schwarz, K.; Luitz, G.K.H.M.D.K.J.; Tran, R.L.F.; Marks, L.D. An Augmented Plane Wave Plus Local Orbitals Program for Calculating Crystal Properties, 3rd-9501031st-ed.; Schwarz, K., Ed.; Vienna University of

Technology: Vienna, Austria, 2019; Volume 2, ISBN 3-9501031-1-2.

31. F. Tran, P. Blaha, Accurate band gaps of semiconductors and insulators with a semilocal exchange-correlation potential, Phys. Rev. letters 102 (2009) 226401.
32. J.L. Erskine, E.A. Stern, Phys. Rev. Lett. 30 (1973) 1329.
33. F. Wooten, Optical Properties of Solids. Academic Press, New York (1972).
34. S. Zhao, C. Lan, J. Ma, S.S Pandey, S. Hayase, T. Ma, First principles study on the electronic and optical properties of B-site ordered double perovskites Sr_2MMoO_6 (M=Mg, Ca and Zn) Solid StateCommun. 19 (2015) 213.
35. G.K.H. Madsen, K. Schwarz, D.J. Singh, BoltzTraP. A code forcalculating band-structure dependent quantities. Comput. Phys. Commun. 175 (2006) 67.
36. G.K.H.Madsen, P. Blaha, K. Schwarz, E. Sjöstedt, L. Nordstrom, efficient linearization of the augmented plane-wave method Phys. Rev. B. 64 (2001) 195134.
37. S. Azam, S. A. Khan, S. Goumri-said, Mater. Res. Bull. 2015, 70, 847.
38. T.T. Khan, S. Ur, Thermoelectric Properties of the Perovskite-Type Oxide $SrTi_{1-x}Nb_xO_3$ Synthesized by Solid-State Reaction Method. Electron. Mater. Lett. 14 (2018) 336.
39. K. Kurosaki, T. Oyama, H. Muta, M. Uno, S. Yamanaka, Thermoelectric properties of perovskite type barium molybdate J. Alloy Compd. 372 (2004) 65.